Subwavelength localized modes for acoustic waves in bubbly crystals with a defect

H. Ammari and B. Fitzpatrick and E. Ovehed Hiltunen and S. Yu

Subwavelength localized modes for acoustic waves in bubbly crystals with a defect

Habib Ammari[*]   Brian Fitzpatrick[*]   Erik Orvehed Hiltunen[†]   Sanghyeon Yu[*]

Abstract

The ability to control wave propagation is of fundamental interest in many areas of physics. Photonic and phononic crystals proved very useful for this purpose but, because they are based on Bragg interferences, these artificial media require structures with large dimensions. In [Ammari et al., Subwavelength phononic bandgap opening in bubbly media, J. Diff. Eq., 263 (2017), 5610–5629], it has been proved that a subwavelength bandgap opening occurs in bubble phononic crystals. To demonstrate the opening of a subwavelength phononic bandgap, a periodic arrangement of bubbles is considered and their subwavelength Minnaert resonance is exploited. In this paper, this subwavelength bandgap is used to demonstrate cavities, very similar to those obtained in photonic and phononic crystals, albeit of deeply subwavelength dimensions. The key idea is to increase the size of a single bubble inside the crystal, thus creating a defect. The goal is then to analytically and numerically show that this crystal has a localized eigenmode close to the defect bubble.

Mathematical Subject Classification (MSC2000). 35R30, 35C20.

Keywords. bubble, subwavelength resonance, subwavelength phononic crystal, subwavelength cavity.

1   Introduction

It is well-known in solid state physics that the periodicity of atoms composing crystals is responsible for the existence of both conducting bands and bandgaps for electrons. This property is a consequence of the Floquet-Bloch theory applied to the wavefunction of electrons. Similarly, electromagnetic and elastic waves propagating in periodic media are subject to the same formalism giving rise to the existence of ranges of frequencies for which no propagation is allowed, so called bandgaps. Such materials are known as photonic and phononic crystals. At an interface with free space, these types of crystals act as mirrors for incoming waves, termed Bragg mirrors. Similarly, a point defect can be created by locally modifying the properties of a crystal. This results in a cavity if the mode supported by the defect is resonant within the bandgap. Physically, the underlying mechanism is Bragg interference. In these periodic media, the Bragg condition typically occurs when the period of the medium scales with the wavelength [5, 6, 7, 17, 23, 19, 30, 31]. As a consequence, photonic and phononic crystals are typically structured with a period corresponding to half the operating wavelength. This constrains the range of applications, specifically in low-frequency regimes where the wavelength is large [33, 36].

Based on the phenomenon of subwavelength resonance, a class of phononic crystals that exhibit bandgaps with deep subwavelength spatial scales have been fabricated [32]. In [3], the opening of a subwavelength phononic bandgap in bubbly crystals has been proved. This subwavelength bandgap is mainly due to the cell resonance of the bubbles in the quasi-static regime and is quite different from the usual bandgaps in photonic/phononic crystals where the gap opens at wavelengths which, as mentioned previously, are comparable to the period of the structure. In [8], it has been further proved that the first Bloch eigenvalue achieves its maximum at the corner of the Brillouin zone. Moreover, by computing the asymptotic of the Bloch eigenfunctions in the periodic structure near that critical frequency, it has been demonstrated that these eigenfunctions can be decomposed into two parts: one which is slowly varying and satisfies a homogenized equation, while the other is periodic across each elementary crystal cell and is varying more rapidly. The asymptotic analysis of wave fields near the critical frequency where a subwavelength bandgap opens rather than the zero frequency has been performed. This rigorously

---

[*]Department of Mathematics, ETH Zürich, Rämistrasse 101, CH-8092 Zürich, Switzerland (habib.ammari@math.ethz.ch, brian.fitzpatrick@sam.math.ethz.ch, sanghyeon.yu@sam.math.ethz.ch).

[†]Engineering physics, Uppsala University, Sweden (Erik.Orvehed_Hiltunen.0207@student.uu.se).

justifies the observed superfocusing of acoustic waves in bubbly crystals near and below the maximum of the first Bloch eigenvalue and confirms the bandgap opening near and above this critical frequency. We refer the reader to [2, 9, 10] for the mathematical analysis of the superfocusing phenomenon in resonant media.

Bubbly media is a natural model for the control of wave propagation at the deep subwavelength scale because of the simplicity of the constituent resonant structure, the air bubbles. It has been known that a single bubble in water possesses a subwavelength resonance which is called the Minnaert resonance [1, 34]. This resonance is due to the high contrast in density between the bubble and the surrounding medium and it makes the air bubble an ideal subwavelength resonator (the bubble can be two order of magnitude smaller than the wavelength at the resonant frequency).

In phononic crystals, a point defect can be created by locally removing a scatterer. This results in a small cavity because a resonant mode is created by the defect within the bandgap [12, 13, 14, 15, 20, 21, 26, 27]. Following this concept, many components have been demonstrated based on periodic media such as waveguides using line defects [11, 28]. However, because of their wavelength scale period, phononic crystals result in relatively large devices. This seriously constrains the range of applications, especially in the low frequency regime where the wavelength is large.

If we remove one bubble inside the bubbly crystal, we cannot create a defect mode. The defect created in this fashion is actually too small to support a resonant mode, while in a phononic crystal removing one scatterer allows for the existence of a stationary defect mode since the typical scale of such a defect is the wavelength. This illustrates a strong difference between Bragg bandgaps and subwavelength bandgaps in bubbly crystals.

In order to tackle this issue, we have to physically introduce a resonant defect inside the crystal of subwavelength resonators, and this is achieved by simply detuning one resonator with respect to the rest of the medium. In the case of the bubbly medium, we prove in this paper that by increasing the radius of one bubble we create a detuned resonator with a resonance frequency that is upward shifted, thus falling within the subwavelength bandgap.

The aim of this paper is to prove the existence of this defect mode. Through the application of layer potential techniques, Floquet-Bloch theory, and Gohberg-Sigal theory we derive an original formula for the defect mode frequency, along with proving the existence of a subwavelength localized mode. Our results are complemented by several numerical examples which serve to validate them in two dimensions. Our results formally explain the experimental observations reported in [24, 25] in the case of Helmholtz resonators. They pave the mathematical foundation for the analysis of wave propagation control the deeply subwavelength scale. Subwavelength cavities have a high quality factor and a low mode volume. These two effects are typically associated with the enhancement of the emission rate of an emitter or the so-called Purcell factor [35].

The paper is organized as follows. In Section 2 we formulate the spectral problem for a bubble phononic crystal and introduce some basic results regarding the quasi-periodic Green's function, stability of the essential spectrum, and Floquet-Bloch theory. In Section 3 we use the fictitious source superposition method introduced in [37] for modelling the defect and characterize the fictitious sources as the solution of some system of integral equations. In section 4, we prove existence of a localized defect mode and derive an asymptotic formula for the resonant frequency created inside the subwavelength bandgap by increasing the size of a single bubble in terms of the ratio between its radius and the radius of the original bubbles. In Section 5 we perform numerical simulations to illustrate the main findings of this paper. We make use of the multipole expansion method to compute the defect mode inside the subwavelength bandgap. The paper ends with some concluding remarks.

2 Preliminaries

2.1 Layer potentials

Let Γ^0 and $\Gamma^k, k > 0$ be the fundamental solution of the Laplace and Helmholtz equations in dimension two, respectively, *i.e.*,

$$
\begin{cases}
\Gamma^k(x,y) = -\dfrac{i}{4} H_0^{(1)}(k|x-y|), & k > 0, \\[2mm]
\Gamma^0(x,y) = \dfrac{1}{2\pi} \ln|x-y|,
\end{cases}
$$

where $H_0^{(1)}$ is the Hankel function of the first kind and order zero.

Let $\mathcal{S}_D^k : L^2(\partial D) \to H^1_{\text{loc}}(\mathbb{R}^2)$ be the single layer potential defined by

$$\mathcal{S}_D^k[\phi](x) = \int_{\partial D} \Gamma^k(x,y)\phi(y)\,d\sigma(y), \quad x \in \mathbb{R}^2.$$

We also define the Neumann-Poincaré operator $\left(\mathcal{K}_D^k\right)^* : L^2(\partial D) \to L^2(\partial D)$ by

$$\left(\mathcal{K}_D^k\right)^* = \int_{\partial D} \frac{\partial}{\partial \nu_x} \Gamma^k(x,y)\phi(y)\,d\sigma(y), \quad x \in \partial D.$$

In the case when $k = 0$, we will omit the superscripts and write $\mathcal{S}_D$ and $\mathcal{K}_D^*$, respectively. The following so-called jump relations of $\mathcal{S}_D^k$ on the boundary ∂D are well-known (see, for instance, [6]):

$$\left.\mathcal{S}_D^k[\phi]\right|_+ = \left.\mathcal{S}_D^k[\phi]\right|_-,$$

and

$$\left.\frac{\partial}{\partial \nu}\mathcal{S}_D^k[\phi]\right|_{\pm} = \left(\pm\frac{1}{2}I + \left(\mathcal{K}_D^k\right)^*\right)[\phi].$$

Here, $\partial/\partial\nu$ denotes the outward normal derivative, and $|_{\pm}$ denotes the limits from outside and inside D.

We also introduce a quasi-periodic version of the layer potentials. Let Y be the unit cell $[-1/2, 1/2]^2$ in $\mathbb{R}^2$. For $\alpha \in [0, 2\pi)^2$, the function $\Gamma^{\alpha,k}$ is defined to satisfy

$$(\triangle_x + k^2)\Gamma^{\alpha,k}(x,y) = \sum_{n\in\mathbb{R}^2} \delta(x - y - n)e^{in\cdot\alpha},$$

where δ is the Dirac delta function and $\Gamma^{\alpha,k}$ is α-quasi-periodic, i.e., $e^{-i\alpha\cdot x}\Gamma^{\alpha,k}(x,y)$ is periodic in x with respect to Y.

We define the quasi-periodic single layer potential $\mathcal{S}_D^{\alpha,k}$ by

$$\mathcal{S}_D^{\alpha,k}[\phi](x) = \int_{\partial D} \Gamma^{\alpha,k}(x,y)\phi(y)d\sigma(y), \quad x \in \mathbb{R}^2.$$

It satisfies the following jump formulas:

$$\left.\mathcal{S}_D^{\alpha,k}[\phi]\right|_+ = \left.\mathcal{S}_D^{\alpha,k}[\phi]\right|_-,$$

and

$$\left.\frac{\partial}{\partial \nu}\right|_{\pm} \mathcal{S}_D^{\alpha,k}[\phi] = \left(\pm\frac{1}{2}I + (\mathcal{K}_D^{-\alpha,k})^*\right)[\phi] \quad \text{on } \partial D,$$

where $(\mathcal{K}_D^{-\alpha,k})^*$ is the operator given by

$$(\mathcal{K}_D^{-\alpha,k})^*[\phi](x) = \text{p.v.} \int_{\partial D} \frac{\partial}{\partial \nu_x} \Gamma^{\alpha,k}(y,y)\phi(y)d\sigma(y).$$

We remark that it is known that $\mathcal{S}_D^{\alpha,0} : L^2(\partial D) \to H^1(\partial D)$ is invertible for $\alpha \neq 0$ [6].

2.2 Floquet transform

A function $f(x)$ is said to be α-quasi-periodic in the variable $x \in \mathbb{R}^2$ if $e^{-i\alpha\cdot x}f(x)$ is periodic. Given a function $f \in L^2(\mathbb{R}^2)$, the Floquet transform is defined as

$$\mathcal{F}[f](x,\alpha) = \sum_{m\in\mathbb{Z}^2} f(x - m)e^{i\alpha\cdot m}, \tag{1}$$

which is α-quasi-periodic in x and periodic in α. Let $Y = [-1/2, 1/2)^2$ be the unit cell and $BZ := \mathbb{R}^2/2\pi\mathbb{Z}^2 \simeq [0, 2\pi)^2$ be the so-called first Brillouin zone. The Floquet transform is an invertible map $\mathcal{F} : L^2(\mathbb{R}^2) \to L^2(Y \times BZ)$, with inverse (see, for instance, [22, 6])

$$\mathcal{F}^{-1}[g](x) = \frac{1}{(2\pi)^2} \int_{BZ} g(x,\alpha)\,d\alpha.$$

2.3 Bubbly crystals and subwavelength bandgaps

Here we briefly review the subwavelength bandgap opening of a bubbly crystal from [3].

Assume that a single bubble occupies D, which is a disk of radius $R < 1/2$ centered at the origin. We denote by ρ_b and κ_b the density and the bulk modulus of the air inside the bubble, respectively. We let ρ_w and κ_w be the corresponding parameters for the water. We introduce

$$v_w = \sqrt{\frac{\kappa_w}{\rho_w}}, \quad v_b = \sqrt{\frac{\kappa_b}{\rho_b}}, \quad k_w = \frac{\omega}{v_w} \quad \text{and} \quad k_b = \frac{\omega}{v_b}$$

to be the speed of sound outside and inside the bubbles, and the wavenumber outside and inside the bubbles, respectively. ω corresponds to the operating frequency of acoustic waves. We also introduce two dimensionless contrast parameters

$$\delta = \frac{\rho_b}{\rho_w} \quad \text{and} \quad \tau = \frac{k_b}{k_w} = \frac{v_w}{v_b} = \sqrt{\frac{\rho_b \kappa_w}{\rho_w \kappa_b}}.$$

We assume that the wave speeds outside and inside the bubbles are comparable to each other and that there is a large contrast in the bulk modulii, that is,

$$\delta \ll 1, \quad \tau = O(1).$$

In this paper, for the sake of simplicity of presentation, we shall assume $v_w = v_b = 1$.

Let $\mathcal{C} = \cup_{n \in \mathbb{Z}^2}(D+n)$ be the periodic bubbly crystal. Consider the following quasi-periodic scattering problem:

$$
\begin{cases}
\nabla \cdot \dfrac{1}{\rho_w} \nabla v + \dfrac{\omega^2}{\kappa_w} v = 0 \quad \text{in} \quad Y \backslash \overline{D}, \\[2mm]
\nabla \cdot \dfrac{1}{\rho_b} \nabla v + \dfrac{\omega^2}{\kappa_b} v = 0 \quad \text{in} \quad D, \\[2mm]
v|_+ - v|_- = 0 \quad \text{on} \quad \partial D, \\[2mm]
\dfrac{1}{\rho_w} \dfrac{\partial v}{\partial \nu}\bigg|_+ - \dfrac{1}{\rho_b} \dfrac{\partial v}{\partial \nu}\bigg|_- = 0 \quad \text{on} \quad \partial D, \\[2mm]
e^{-i\alpha \cdot x} v \text{ is periodic.}
\end{cases}
\tag{2}
$$

It is known that (2) has nontrivial solutions for discrete values of ω such as

$$0 \leq \omega_1^\alpha \leq \omega_2^\alpha \leq \cdots$$

and thus we have the following band structure of propagating frequencies for the periodic bubbly crystal $\mathcal{C}$:

$$[0, \max_\alpha \omega_1^\alpha] \cup [\min_\alpha \omega_2^\alpha, \max_\alpha \omega_2^\alpha] \cup \cdots .$$

In [3], it is proved that there exists a subwavelength spectral gap opening in the band structure. Let us briefly review this result. We look for a solution of (2) which has the following form:

$$
v =
\begin{cases}
\mathcal{S}_D^{\alpha, k_w}[\varphi^\alpha] & \text{in } Y \setminus \bar{D}, \\[2mm]
\mathcal{S}_D^{k_b}[\psi^\alpha] & \text{in } D,
\end{cases}
\tag{3}
$$

for some densities $\varphi^\alpha, \psi^\alpha \in L^2(\partial D)$. Using the jump relations for the single layer potentials, one can show that (2) is equivalent to the boundary integral equation

$$\mathcal{A}^\alpha(\omega, \delta)[\Phi^\alpha] = 0, \tag{4}$$

where

$$\mathcal{A}^\alpha(\omega, \delta) = \begin{pmatrix} \mathcal{S}_D^{k_b} & -\mathcal{S}_D^{\alpha, k} \\ -\frac{1}{2} + \mathcal{K}_D^{k_b, *} & -\delta(\frac{1}{2} + (\mathcal{K}_D^{-\alpha, k})^*) \end{pmatrix}, \quad \Phi^\alpha = \begin{pmatrix} \varphi^\alpha \\ \psi^\alpha \end{pmatrix}.$$

Since it can be shown that $\omega = 0$ is a characteristic value for the operator-valued analytic function $\mathcal{A}(\omega, 0)$, we can conclude the following result by the Gohberg-Sigal theory [6, 18].

Lemma 1. *For any δ sufficiently small, there exists a characteristic value $\omega_1^\alpha = \omega_1^\alpha(\delta)$ to the operator-valued analytic function $\mathcal{A}^\alpha(\omega, \delta)$ such that $\omega_1^\alpha(0) = 0$ and ω_1^α depends on δ continuously.*

The next theorem gives the asymptotic expansion of ω_1^α as $\delta \to 0$.

Theorem 1. [3] *For $\alpha \neq 0$ and sufficiently small δ, we have*

$$\omega_1^\alpha = \omega_M \sqrt{\frac{\mathrm{Cap}_{D,\alpha}}{\mathrm{Cap}_D}} + O(\delta^{3/2}), \tag{5}$$

where the constants $\mathrm{Cap}_{D,\alpha}$ and Cap_D are given by

$$\mathrm{Cap}_{D,\alpha} := -((\mathcal{S}_D^{\alpha,0})^{-1}[\chi_{\partial D}], \chi_{\partial D}), \quad \mathrm{Cap}_D = -\frac{2\pi}{\ln R},$$

and ω_M is the (free space) Minnaert resonant frequency satisfying $(\omega_M)^2 \ln \omega_M = O(\delta)$ as $\delta \to 0$.

Let $\omega_1^* = \max_\alpha \omega_1^\alpha$. The following theorem specifies the subwavelength bandgap opening.

Theorem 2. [3] *For every $\varepsilon > 0$, there exists $\delta_0 > 0$ and $\tilde{\omega} > \omega_1^*$ such that*

$$[\omega_1^* + \varepsilon, \tilde{\omega}] \subset [\max_\alpha \omega_1^\alpha, \min_\alpha \omega_2^\alpha] \tag{6}$$

for $\delta < \delta_0$.

3 Integral representation for bubbly crystals with a defect

3.1 Bubbly crystals with a defect: problem formulation

Consider now a perturbed crystal, where the central disk D is replaced by a defect disk D_d of radius R_d with $R < R_d < 1/2$. Let $\mathcal{C}_d = D_d \cup \left(\cup_{n \in \mathbb{Z}^2 \backslash \{0,0\}} D + n \right)$ be the perturbed crystal and let $\varepsilon = R_d - R > 0$ be the perturbation of the radius. We consider the following problem:

$$\begin{cases} \nabla \cdot \dfrac{1}{\rho_w} \nabla u + \dfrac{\omega^2}{\kappa_w} u = 0 & \text{in} \quad \mathbb{R}^2 \backslash \mathcal{C}_d, \\[2mm] \nabla \cdot \dfrac{1}{\rho_b} \nabla u + \dfrac{\omega^2}{\kappa_b} u = 0 & \text{in} \quad \mathcal{C}_d, \\[2mm] u|_+ - u|_- = 0 & \text{on} \quad \partial \mathcal{C}_d, \\[2mm] \dfrac{1}{\rho_w} \dfrac{\partial u}{\partial \nu}\bigg|_+ - \dfrac{1}{\rho_b} \dfrac{\partial u}{\partial \nu}\bigg|_- = 0 & \text{on} \quad \partial \mathcal{C}_d. \end{cases} \tag{7}$$

As discussed in Subsection 2.3, the unperturbed problem (with $\mathcal{C}$ instead of $\mathcal{C}_d$ in (7)), has the following essential spectrum for the propagating frequencies:

$$[0, \max_\alpha \omega_1^\alpha] \cup [\min_\alpha \omega_2^\alpha, \max_\alpha \omega_2^\alpha] \cup \cdots.$$

In fact, it can be easily shown that the perturbed crystal problem (7) has the same essential spectrum. This is because the essential spectrum is stable under compact perturbations [16].

In this paper, we want to show that by modifying the central bubble D, there exists a frequency ω^ε, slightly above $\max_\alpha \omega_1^\alpha$, which results in a non-trivial solution to the problem (7). The solution u associated with the frequency ω^ε should be localized since ω^ε lies in the bandgap. Moreover, it is of a subwavelength nature.

3.2 Effective sources for the defect

It is difficult to obtain the boundary integral formulation of the problem (7) directly. Here we consider the effective source solution which models the defect D_d by placing non-trivial sources onto the boundary of the central bubble D of the unperturbed crystal $\mathcal{C}$. Since the geometry of the unperturbed crystal is periodic, we can use the Floquet-Bloch theory. This is motivated by the fictitious source superposition method introduced in [37].

Let us consider the following problem:

$$
\begin{cases}
\nabla \cdot \dfrac{1}{\rho_w}\nabla \tilde{u} + \dfrac{\omega^2}{\kappa_w}\tilde{u} = 0 & \text{in} \quad \mathbb{R}^2 \setminus \mathcal{C}, \\[2mm]
\nabla \cdot \dfrac{1}{\rho_b}\nabla \tilde{u} + \dfrac{\omega^2}{\kappa_b}\tilde{u} = 0 & \text{in} \quad \mathcal{C}, \\[2mm]
\tilde{u}|_+ - \tilde{u}|_- = f\delta_{m,(0,0)} & \text{on} \quad \partial D + m, \; m \in \mathbb{Z}^2, \\[2mm]
\dfrac{1}{\rho_w}\dfrac{\partial \tilde{u}}{\partial \nu}\bigg|_+ - \dfrac{1}{\rho_b}\dfrac{\partial \tilde{u}}{\partial \nu}\bigg|_- = g\delta_{m,(0,0)} & \text{on} \quad \partial D + m, \; m \in \mathbb{Z}^2.
\end{cases}
\tag{8}
$$

where f, g are the source terms and $\delta_{m,n}$ is the Kronecker delta function. Note that the non-zero sources are present only on the boundary of the central bubble D.

If the source terms f and g satisfy some appropriate conditions, then we will have

$$
u \equiv \tilde{u} \quad \text{in} \ (\mathbb{R}^2 \setminus D_d) \cup D.
$$

Once this is achieved, the original solution u can be recovered by extending the solution $\tilde{u}$ to the whole region including $D_d \setminus D$ with boundary conditions on ∂D and ∂D_d. The conditions for the effective sources f and g, which are necessary in order to correctly model the defect, will be characterized in the next subsection.

3.3 Characterization of the effective sources

Here we clarify the relation between the effective source pair (f, g) and the density pair (φ, ψ).

First we consider the integral equation for the solution $\tilde{u}$ inside the central unit cell Y. Inside Y, the solution $\tilde{u}$ can be represented as

$$
\tilde{u} =
\begin{cases}
H + \mathcal{S}_D^{k_w}[\psi] & \text{in } Y \setminus \overline{D}, \\[1mm]
\mathcal{S}_D^{k_b}[\varphi] & \text{in } D.
\end{cases}
\tag{9}
$$

Here, the pair $(\varphi, \psi) \in L^2(\partial D)^2$ satisfies

$$
\mathcal{A}_D \begin{pmatrix} \varphi \\ \psi \end{pmatrix} :=
\begin{pmatrix}
\mathcal{S}_D^{k_b} & -\mathcal{S}_D^{k_w} \\[1mm]
\partial_\nu \mathcal{S}_D^{k_b}|_- & -\delta \partial_\nu \mathcal{S}_D^{k_w}|_+
\end{pmatrix}
\begin{pmatrix} \varphi \\ \psi \end{pmatrix} =
\begin{pmatrix} H|_{\partial D} - f \\ \partial_\nu H|_{\partial D} - g \end{pmatrix}.
\tag{10}
$$

Next, let us consider the central cell Y in the original problem (7). The central cell Y contains a defect bubble D_d and no sources. Inside Y, the solution u is represented as

$$
u =
\begin{cases}
H + \mathcal{S}_{D_d}^{k_w}[\psi_d] & \text{in } Y \setminus \overline{D_d}, \\[1mm]
\mathcal{S}_{D_d}^{k_b}[\varphi_d] & \text{in } D_d,
\end{cases}
$$

where

$$
\mathcal{A}_{D_d} \begin{pmatrix} \varphi_d \\ \psi_d \end{pmatrix} :=
\begin{pmatrix}
\mathcal{S}_{D_d}^{k_b} & -\mathcal{S}_{D_d}^{k_w} \\[1mm]
\partial_\nu \mathcal{S}_{D_d}^{k_b}|_- & -\delta \partial_\nu \mathcal{S}_{D_d}^{k_w}|_+
\end{pmatrix}
\begin{pmatrix} \varphi_d \\ \psi_d \end{pmatrix} =
\begin{pmatrix} H|_{\partial D_d} \\ \partial_\nu H|_{\partial D_d} \end{pmatrix}.
\tag{11}
$$

In order for the effective sources f and g to model the defect D_d correctly, we should impose $u \equiv \tilde{u}$ in $(Y \setminus D_d) \cup D$. In other words, the following conditions should be satisfied:

$$
\mathcal{S}_{D_d}^{k_b}[\varphi_d] \equiv \mathcal{S}_D^{k_b}[\varphi] \quad \text{in } D_d,
\tag{12}
$$

and

$$
\mathcal{S}_{D_d}^{k_w}[\psi_d] \equiv \mathcal{S}_D^{k_w}[\psi] \quad \text{in } Y \setminus \overline{D}.
\tag{13}
$$

Since D and D_d are circular disks, we can use a Fourier basis for functions on ∂D or ∂D_d in polar coordinates (r, θ) to make (11)-(13) more explicit. Let us write φ and ψ in the form of Fourier series:

$$
\varphi(\theta) = \sum_{n \in \mathbb{Z}} \varphi_n e^{in\theta}, \quad \psi(\theta) = \sum_{n \in \mathbb{Z}} \psi_n e^{in\theta}.
$$

Similarly, we also write φ_d and ψ_d as

$$\varphi_d(\theta) = \sum_{n \in \mathbb{Z}} \varphi_{d,n} e^{in\theta}, \quad \psi_d(\theta) = \sum_{n \in \mathbb{Z}} \psi_{d,n} e^{in\theta}.$$

We define the subspace V_{mn} of $L^2(\partial D)^2$ as

$$V_{mn} := \text{span}\{e^{im\theta}\} \times \text{span}\{e^{in\theta}\}, \quad m, n \in \mathbb{Z}.$$

Similarly, let V_{mn}^d be the subspace of $L^2(\partial D_d)^2$ with the same Fourier basis.

It is known that (see, for instance, [3])

$$\mathcal{S}_D^k[e^{in\theta}] = \frac{(-1)i\pi R}{2} \times \begin{cases} J_n(kR)H_n^{(1)}(kr)e^{in\theta}, & r \geq R, \\ H_n^{(1)}(kR)J_n(kr)e^{in\theta}, & 0 \leq r < R. \end{cases} \tag{14}$$

Therefore, the operator $\mathcal{A}_D$ in (10) has the following matrix representation as an operator from V_{mn} to $V_{m'n'}$:

$$(\mathcal{A}_D)_{V_{mn} \to V_{m'n'}} = \delta_{mn}\delta_{m'n'} \frac{(-i)\pi R}{2} \begin{pmatrix} J_n(k_bR)H_n^{(1)}(k_bR) & -J_n(k_wR)H_n^{(1)}(k_wR) \\ k_bJ_n'(k_bR)H_n^{(1)}(k_bR) & -\delta k_w J_n(k_wR)\big(H_n^{(1)}\big)'(k_wR) \end{pmatrix}. \tag{15}$$

Similarly, the operator $\mathcal{A}_{D_d}$ in (11), as a mapping from V_{mn}^d to $V_{m'n'}^d$, is represented as follows:

$$(\mathcal{A}_{D_d})_{V_{mn}^d \to V_{m'n'}^d} = \delta_{mn}\delta_{m'n'} \frac{(-i)\pi R_d}{2} \begin{pmatrix} J_n(k_bR_d)H_n^{(1)}(k_bR_d) & -J_n(k_wR_d)H_n^{(1)}(k_wR_d) \\ k_bJ_n'(k_bR_d)H_n^{(1)}(k_bR_d) & -\delta k_w J_n(k_wR_d)\big(H_n^{(1)}\big)'(k_wR_d) \end{pmatrix}. \tag{16}$$

Now, we consider (12) and (13). We have from (14) that, inside D_d,

$$\mathcal{S}_D^{k_b}[\varphi_d] = \sum_{n \in \mathbb{Z}} \varphi_n \mathcal{S}_D^{k_b}[e^{in\theta}] = \frac{(-i)\pi R}{2} \sum_{n \in \mathbb{Z}} \varphi_n H_n^{(1)}(k_bR)J_n(k_br)e^{in\theta}$$

$$= \frac{(-i)\pi R}{2} \sum_{n \in \mathbb{Z}} \varphi_n \frac{H_n^{(1)}(k_bR)}{H_n^{(1)}(k_bR_d)} H_n^{(1)}(k_bR)J_n(k_br)e^{in\theta}$$

$$= \mathcal{S}_{D_d}^{k_b}\Big[\sum_{n \in \mathbb{Z}} \varphi_n \frac{H_n^{(1)}(k_bR)}{H_n^{(1)}(k_bR_d)} e^{in\theta}\Big].$$

Similarly, outside D,

$$\mathcal{S}_D^{k_w}[\psi] = \mathcal{S}_{D_d}^{k_w}\Big[\sum_{n \in \mathbb{Z}} \psi_n \frac{J_n(k_wR)}{J_n(k_wR_d)} e^{in\theta}\Big].$$

So, from (12) and (13), we see that

$$\begin{pmatrix} \varphi_d \\ \psi_d \end{pmatrix} = \mathcal{P}_1 \begin{pmatrix} \varphi \\ \psi \end{pmatrix},$$

where the operator $\mathcal{P}_1 : L^2(\partial D)^2 \to L^2(\partial D_d)^2$ is given by

$$(\mathcal{P}_1)_{V_{mn} \to V_{m'n'}^d} = \delta_{mn}\delta_{m'n'} \begin{pmatrix} \dfrac{H_n^{(1)}(k_bR)}{H_n^{(1)}(k_bR_d)} & 0 \\ 0 & \dfrac{J_n(k_wR)}{J_n(k_wR_d)} \end{pmatrix}.$$

In the same way, we can obtain that

$$\begin{pmatrix} H|_{\partial D_d} \\ \partial_\nu H|_{\partial D_d} \end{pmatrix} = \mathcal{P}_2^\varepsilon \begin{pmatrix} H|_{\partial D} \\ \partial_\nu H|_{\partial D} \end{pmatrix},$$

where the operator $\mathcal{P}_2 : L^2(\partial D)^2 \to L^2(\partial D_d)^2$ is given by

$$(\mathcal{P}_2)_{V_n \to V_m^d} = \delta_{mn} \begin{pmatrix} \dfrac{J_n(k_w R_d)}{J_n(k_w R)} & 0 \\ 0 & \dfrac{J_n'(k_w R_d)}{J_n'(k_w R)} \end{pmatrix}.$$

Therefore, using (11), we arrive at

$$\mathcal{A}_D^\varepsilon \begin{pmatrix} \varphi \\ \psi \end{pmatrix} := (\mathcal{P}_2)^{-1} \mathcal{A}_{D_d} \mathcal{P}_1 \begin{pmatrix} \varphi \\ \psi \end{pmatrix} = \begin{pmatrix} H|_{\partial D} \\ \partial_\nu H|_{\partial D} \end{pmatrix}. \tag{17}$$

Thus, (10) yields

$$(\mathcal{A}_D^\varepsilon - \mathcal{A}_D) \begin{pmatrix} \varphi \\ \psi \end{pmatrix} = \begin{pmatrix} f \\ g \end{pmatrix}. \tag{18}$$

We have obtained an explicit relation between the pair (φ, ψ) and the effective sources (f, g). If the effective sources f and g satisfy (18), then the pair (f, g) will result in the generation of the same scattered field as the one induced by the defect bubble D_d. In other words, $\widetilde{u} \equiv u$ outside $D_d \setminus \overline{D}$. In what follows, for convenience of notation, we will identify the solution $\widetilde{u}$ with the original one u.

3.4 Floquet transform of the solution

Here we derive an integral equation for the effective source problem (8). We apply the Floquet transform to the solution u with the quasi-periodic parameter α as follows

$$u^\alpha = \sum_{m \in \mathbb{Z}^2} u(x - m) e^{i\alpha \cdot m}.$$

The transformed solution u^α satisfies

$$\begin{cases} \nabla \cdot \dfrac{1}{\rho_w} \nabla u^\alpha + \dfrac{\omega^2}{\kappa_w} u^\alpha = 0 \quad \text{in} \quad Y \setminus \overline{D}, \\[2mm] \nabla \cdot \dfrac{1}{\rho_b} \nabla u^\alpha + \dfrac{\omega^2}{\kappa_b} u^\alpha = 0 \quad \text{in} \quad D, \\[2mm] u^\alpha|_+ - u^\alpha|_- = f \quad \text{on} \quad \partial D, \\[2mm] \dfrac{1}{\rho_w} \dfrac{\partial u^\alpha}{\partial \nu}\bigg|_+ - \dfrac{1}{\rho_b} \dfrac{\partial u^\alpha}{\partial \nu}\bigg|_- = g \quad \text{on} \quad \partial D, \\[2mm] e^{-i\alpha \cdot x} u^\alpha \text{ is periodic.} \end{cases} \tag{19}$$

The solution u^α can be represented using quasi-periodic layer potentials as

$$u^\alpha = \begin{cases} \mathcal{S}_D^{\alpha, k_w}[\psi_\alpha], & \text{in } Y \setminus \overline{D}, \\ \mathcal{S}_D^{k_b}[\varphi_\alpha], & \text{in } D, \end{cases}$$

where the pair $(\varphi^\alpha, \psi^\alpha) \in L^2(\partial D)^2$ is the solution to

$$\mathcal{A}^\alpha(\omega, \delta) \begin{pmatrix} \varphi^\alpha \\ \psi^\alpha \end{pmatrix} := \begin{pmatrix} \mathcal{S}_D^{k_b} & -\mathcal{S}_D^{\alpha, k_w} \\ \partial_\nu \mathcal{S}_D^{k_b}|_- & -\delta \partial_\nu \mathcal{S}_D^{\alpha, k_w}|_+ \end{pmatrix} \begin{pmatrix} \varphi^\alpha \\ \psi^\alpha \end{pmatrix} = \begin{pmatrix} -f \\ -g \end{pmatrix}. \tag{20}$$

Since the operator $\mathcal{A}_\alpha$ is invertible for small enough ω and δ [3], we have

$$\begin{pmatrix} \varphi^\alpha \\ \psi^\alpha \end{pmatrix} = \mathcal{A}^\alpha(\omega, \delta)^{-1} \begin{pmatrix} -f \\ -g \end{pmatrix}.$$

The original solution u can be recovered by the inversion formula as follows

$$u(x) = \frac{1}{(2\pi)^2} \int_{BZ} u^\alpha(x) d\alpha. \tag{21}$$

8

Then, inside the region D, the solution u satisfies

$$u = \mathcal{S}_D^{k_b}\Big[\frac{1}{(2\pi)^2}\int_{BZ}\varphi^\alpha d\alpha\Big].$$

Similarly, inside the region $Y \setminus \overline{D}$, we have

$$u = \frac{1}{(2\pi)^2}\int_{BZ}\mathcal{S}_D^{\alpha,k_w}[\psi^\alpha]d\alpha = \mathcal{S}_D^{k_w}\Big[\frac{1}{(2\pi)^2}\int_{BZ}\psi^\alpha d\alpha\Big] + \frac{1}{(2\pi)^2}\int_{BZ}\sum_{m\in\mathbb{Z}^2,m\neq 0}\mathcal{S}_D^{k_w}[\psi^\alpha](\cdot - m)e^{im\cdot\alpha}d\alpha.$$

Note that the second term in the right-hand side satisfies the homogeneous Helmholtz equation $(\Delta + k_w^2)u = 0$ in $Y \setminus \overline{D}$. So, in view of (9), we can identify φ, ψ and H as follows:

$$\varphi = \frac{1}{(2\pi)^2}\int_{BZ}\varphi^\alpha d\alpha, \quad \psi = \frac{1}{(2\pi)^2}\int_{BZ}\psi^\alpha d\alpha,$$

and

$$H = \frac{1}{(2\pi)^2}\int_{BZ}\sum_{m\in\mathbb{Z}^2,m\neq 0}\mathcal{S}_D^{k_w}[\psi^\alpha](\cdot - m)e^{im\cdot\alpha}d\alpha.$$

Therefore, from (20), we get the following result.

Propostition 1. *The density pair (φ, ψ) and the effective source pair (f, g) satisfy*

$$\begin{pmatrix}\varphi \\ \psi\end{pmatrix} = \Big(\frac{1}{(2\pi)^2}\int_{BZ}\mathcal{A}^\alpha(\omega,\delta)^{-1}d\alpha\Big)\begin{pmatrix}-f \\ -g\end{pmatrix} \tag{22}$$

for small enough ω and δ.

3.5   The integral equation for the effective sources

Here we derive the integral equation for the effective source pair (f, g). We have the following result.

Propostition 2. *The effective source pair $(f, g) \in L^2(\partial D)^2$ satisfies the following integral equation:*

$$\mathcal{M}^\varepsilon(\omega)\begin{pmatrix}f \\ g\end{pmatrix} := \Big(I + (\mathcal{A}_D^\varepsilon(\omega,\delta) - \mathcal{A}_D(\omega,\delta))\frac{1}{(2\pi)^2}\int_{BZ}\mathcal{A}^\alpha(\omega,\delta)^{-1}d\alpha\Big)\begin{pmatrix}f \\ g\end{pmatrix} = \begin{pmatrix}0 \\ 0\end{pmatrix}. \tag{23}$$

Proof. Applying $\mathcal{A}_{D_d}^{-1}$ to (10), we get

$$\mathcal{A}_{D_d}^{-1}\mathcal{A}_D\begin{pmatrix}\varphi \\ \psi\end{pmatrix} + A_{D_d}^{-1}\begin{pmatrix}f \\ g\end{pmatrix} = \mathcal{A}_{D_d}^{-1}\begin{pmatrix}H|_{\partial D} \\ \partial_\nu H|_{\partial D}\end{pmatrix}.$$

Then, by (17), we have

$$\mathcal{A}_{D_d}^{-1}\mathcal{A}_D\begin{pmatrix}\varphi \\ \psi\end{pmatrix} + A_{D_d}^{-1}\begin{pmatrix}f \\ g\end{pmatrix} = \begin{pmatrix}\varphi \\ \psi\end{pmatrix}.$$

So, from (22), we obtain

$$\Big(\big(-\mathcal{A}_{D_d}^{-1}\mathcal{A}_D + I\big)\Big(\frac{1}{(2\pi)^2}\int_{BZ}(\mathcal{A}^\alpha)^{-1}d\alpha\Big) + \mathcal{A}_{D_d}^{-1}\Big)\begin{pmatrix}f \\ g\end{pmatrix} = \begin{pmatrix}0 \\ 0\end{pmatrix}.$$

Finally, applying $\mathcal{A}_{D_d}$ to the above, we get the desired result. $\qquad\square$

Thus, if we find a value of ω in the bandgap such that there exists a non-trivial solution pair (f, g) to (23), then we have found a resonant frequency for the localized mode.

4 Subwavelength localized modes

4.1 The resonant frequency of the localized mode

Here we prove that a frequency for the localized mode can exist slightly above $\max_\alpha \omega_1^\alpha$. In what follows, let us omit the subscript in ω_1^α for ease of notation. We also do not make explicit the dependence on δ.

We need to study the characteristic value of the operator $\mathcal{M}^\varepsilon$ appearing in (23). Let us first analyze the operator $\int_{BZ}(\mathcal{A}^\alpha)^{-1}d\alpha$. Since ω^α is a simple pole of the mapping $\omega \mapsto \mathcal{A}^\alpha(\omega,)^{-1}$ in a neighborhood of ω^α, according to [6], we can write

$$\mathcal{A}^\alpha(\omega)^{-1} = \frac{\mathcal{L}^\alpha}{\omega - \omega^\alpha} + \mathcal{R}^\alpha(\omega), \tag{24}$$

where the operator-valued function $\mathcal{R}^\alpha(\omega)$ is holomorphic in a neighborhood of ω^α, and the operator $\mathcal{L}^\alpha$ maps $L^2(\partial D)^2$ onto $\ker \mathcal{A}^\alpha(\omega^\alpha, \delta)$. Let us write

$$\ker \mathcal{A}^\alpha(\omega^\alpha) = \mathrm{span}\{\Phi^\alpha\}.$$

Then, again from [6], it can be shown that

$$\mathcal{L}^\alpha = \frac{\langle \Phi^\alpha, \,\cdot\, \rangle \Phi^\alpha}{\langle \Phi^\alpha, \frac{d}{d\omega}\mathcal{A}^\alpha\big|_{\omega=\omega^\alpha}\Phi^\alpha \rangle},$$

where $\langle\,\cdot\,,\,\cdot\,\rangle$ stands for the standard inner product of $L^2(\partial D)^2$.

Hence the operator $\mathcal{M}^\varepsilon$ can be decomposed as

$$\mathcal{M}^\varepsilon = I + (\mathcal{A}_D^\varepsilon - \mathcal{A}_D)\frac{1}{(2\pi)^2}\int_{BZ}\frac{\mathcal{L}^\alpha}{\omega - \omega_\alpha}d\alpha + (\mathcal{A}_D^\varepsilon - \mathcal{A}_D)\frac{1}{(2\pi)^2}\int_{BZ}\mathcal{R}_\alpha d\alpha.$$

Note that the third term in the right-hand side is holomorphic with respect to ω.

Denote by $\alpha^* = (\pi, \pi)$ and $\omega^* = \omega^{(\pi,\pi)}$. In [8], it was proved that, using the symmetry of the square array of bubbles, ω^α attains its maximum at $\alpha = \alpha^*$. Since we are assuming that each bubble is a circular disk, we can derive a slightly more refined result as shown in the following lemma.

Lemma 2. *The characteristic value ω_α attains its maximum at $\alpha = \alpha^*$. Moreover, for α near α_*, we have*

$$\omega^\alpha = \omega^* - \frac{1}{2}c_\delta|\alpha - \alpha_*|^2 + o(|\alpha - \alpha_*|^2).$$

Here, c_δ is a positive constant depending on δ.

In view of the above lemma, we can expect that the operator $\int_{BZ}\frac{\mathcal{L}^\alpha}{\omega - \omega^\alpha}$ becomes singular when $\omega \to \omega^*(= \max_\alpha \omega^\alpha)$. Let us extract its singular part explicitly. Before doing this, we introduce some notations. Denote by $\mathcal{A}^* = \mathcal{A}^{(\pi,\pi)}$, $\Phi^* = \Phi^{(\pi,\pi)}$, and $\mathcal{L}^* = \mathcal{L}^{(\pi,\pi)}$. We also define a small neighborhood V of ω^* which excludes the real interval $(-\infty, \omega^*]$, namely,

$$V = \{|\omega - \omega^*| < r_*\} \setminus (-\infty, \omega^*],$$

for some small enough $r_* > 0$. By Lemma 2, we have

$$\frac{1}{(2\pi)^2}\int_{BZ}\frac{\mathcal{L}^\alpha}{\omega - \omega^\alpha}d\alpha = \mathcal{L}^*\frac{1}{(2\pi)^2}\int_{BZ}\frac{1}{\omega - \omega^* + \frac{1}{2}c_\delta|\alpha - \alpha^*|^2}d\alpha + b_1(\omega)$$

$$= \mathcal{L}^*\frac{1}{(2\pi)^2}\int_{|\alpha-\alpha^*|<1}\frac{1}{\omega - \omega^* + \frac{1}{2}c_\delta|\alpha - \alpha^*|^2}d\alpha + b_2(\omega).$$

Hereafter, b_j means a bounded function with respect to ω in V. Then, using the polar coordinates $\alpha - \alpha_* = (r', \theta')$, we get

$$\frac{1}{(2\pi)^2}\int_{BZ}\frac{\mathcal{L}^\alpha}{\omega - \omega^\alpha}d\alpha = \frac{1}{(2\pi)^2}\int_0^1\frac{2\pi r'}{\omega - \omega_* + \frac{1}{2}c_\delta r'^2}dr' + b_2(\omega)$$

$$= \frac{1}{2\pi c_\delta}\ln(\omega - \omega_*) + b_3(\omega).$$

Here, the usual principal branch is taken for the logarithm and so the operator $\int_{BZ} \frac{\mathcal{L}^\alpha}{\omega - \omega^\alpha} d\alpha$ has a branch cut on $(-\infty, \omega^*]$. We also observe that, for $\omega \in V$,

$$\ln(\omega - \omega^*)(\mathcal{A}_D^\varepsilon(\omega) - \mathcal{A}_D(\omega)) = \ln(\omega - \omega^*)(\mathcal{A}_D^\varepsilon(\omega^*) - \mathcal{A}_D(\omega)^*) + b_4(\omega).$$

Therefore, the integral equation (23) can be rewritten as

$$\mathcal{M}^\varepsilon(\omega) \begin{pmatrix} f \\ g \end{pmatrix} = \left(I + \frac{\ln(\omega - \omega^*)}{2\pi c_\delta}(\mathcal{A}_D^\varepsilon(\omega^*) - \mathcal{A}_D(\omega^*))\mathcal{L}^* + \mathcal{R}^\varepsilon(\omega) \right) \begin{pmatrix} f \\ g \end{pmatrix} = \begin{pmatrix} 0 \\ 0 \end{pmatrix},$$

where $\mathcal{R}^\varepsilon$ is analytic and bounded with respect to ω in V and satisfies $\mathcal{R}^\varepsilon = O(\varepsilon)$. We first consider the principal part $\mathcal{N}^\varepsilon(\omega)$, namely,

$$\mathcal{N}^\varepsilon : \omega \mapsto \mathcal{N}^\varepsilon(\omega) = I + \frac{1}{2\pi c_\delta} \log(\omega - \omega^*)(\mathcal{A}_D^\varepsilon(\omega^*) - \mathcal{A}_D(\omega^*))\mathcal{L}^*.$$

Let us find its characteristic value $\widehat{\omega}$, i.e., $\widehat{\omega} \in V$ such that there exists a nontrivial function $\widehat{\Phi}$ satisfying $\mathcal{N}^\varepsilon(\widehat{\omega})\widehat{\Phi} = 0$. Equivalently, we have

$$\widehat{\Phi} + \frac{1}{2\pi c_\delta} \log(\widehat{\omega} - \omega^*) \frac{(\mathcal{A}_D^\varepsilon - \mathcal{A}_D)(\omega^*)\Phi^*}{\langle \Phi^*, \frac{d}{d\omega}\mathcal{A}^* |_{\omega=\omega^*} \Phi^* \rangle} \langle \Phi^*, \widehat{\Phi} \rangle = 0.$$

Then, by multiplying by Φ^*,

$$\langle \Phi^*, \widehat{\Phi} \rangle \left(1 + \frac{1}{2\pi c_\delta} \log(\widehat{\omega} - \omega^*) \frac{\langle \Phi^*, (\mathcal{A}_D^\varepsilon - \mathcal{A}_D)(\omega^*)\Phi^* \rangle}{\langle \Phi^*, \frac{d}{d\omega}\mathcal{A}^* |_{\omega=\omega^*} \Phi^* \rangle} \right) = 0.$$

Since $\langle \Phi^*, \widehat{\Phi} \rangle = 0$ would imply $\widehat{\Phi} = 0$, we get

$$1 + \frac{1}{2\pi c_\delta} \log(\widehat{\omega} - \omega^*) \frac{\langle \Phi^*, (\mathcal{A}_D^\varepsilon - \mathcal{A}_D)(\omega^*)\Phi^* \rangle}{\langle \Phi^*, \frac{d}{d\omega}\mathcal{A}^* |_{\omega=\omega^*} \Phi^* \rangle} = 0. \tag{25}$$

Before solving the above equation for ω, we need the following lemmas whose proofs will be given in Subsection 4.2.

Lemma 3. *The following results hold:*

(i) For small enough δ, we have

$$\left\langle \Phi^*, \frac{d}{d\omega}\mathcal{A}^*(\omega^*, \delta)\Phi^* \right\rangle \approx -\omega^* \ln \omega^* \frac{R^2}{2} > 0.$$

(ii) For small enough δ and ε, we have

$$\left\langle \Phi^*, \left(\mathcal{A}_D^\varepsilon(\omega^*, \delta) - \mathcal{A}_D(\omega^*, \delta) \right)\Phi^* \right\rangle \approx 4\pi\varepsilon \left(-\frac{R^2}{2}(\omega^*)^2 \ln \omega^* + \delta \right) > 0.$$

In view of Lemma 3, we see from (25) that

$$\widehat{\omega} - \omega_* = \exp\left(-2\pi c_\delta \left\langle \Phi^*, \frac{d}{d\omega}\mathcal{A}^*(\omega^*)\Phi^* \right\rangle \left\langle \Phi^*, \left(\mathcal{A}_D^\varepsilon(\omega^*) - \mathcal{A}_D(\omega^*) \right)\Phi^* \right\rangle^{-1} \right).$$

We can also see that the right-hand side is positive and goes to zero as ε tends to zero. In other words, $\widehat{\omega} \to \omega^*$ as $\varepsilon \to 0$. Now we turn to the full operator $\mathcal{M}^\varepsilon$. Recall that $\mathcal{M}^\varepsilon = \mathcal{N}^\varepsilon + \mathcal{R}^\varepsilon$ and $\mathcal{R}^\varepsilon$ is holomorphic, bounded and satisfies $\mathcal{R}^\varepsilon = O(\varepsilon)$ in V. So by Gohberg-Sigal theory [6], we can conclude that there exists a characteristic value ω^ε of the operator-valued function $\mathcal{M}^\varepsilon$ near ω^*. Let us denote its associated root function by Φ^ε. We choose Φ^ε so that $\langle \Phi^*, \Phi^\varepsilon \rangle = 1$. Then, as in the derivations of (25), we can obtain

$$1 + \frac{1}{2\pi c_\delta} \log(\widehat{\omega} - \omega^*) \frac{\langle \Phi^*, (\mathcal{A}_D^\varepsilon - \mathcal{A}_D)(\omega^*)\Phi^* \rangle}{\langle \Phi^*, \frac{d}{d\omega}\mathcal{A}^* |_{\omega=\omega^*} \Phi^* \rangle} + \langle \Phi^*, \mathcal{R}^\varepsilon(\omega)\Phi^\varepsilon \rangle = 0.$$

Note that $\langle \Phi^*, \mathcal{R}^\varepsilon(\omega)\Phi^\varepsilon \rangle = O(\varepsilon)$.

Therefore, we have proved the following theorem which is the main result of this paper.

11

Theorem 3. *For small enough ε and δ, there exists one frequency value ω^ε such that the problem (7) has a nontrivial solution and ω^ε is slightly above ω^*. Moreover, we have*

$$\omega^\varepsilon - \omega_* = \exp\Big(-\frac{c_\delta}{2\varepsilon}\frac{\frac{R^2}{2}\omega^*(-\ln\omega^*)}{(\frac{R^2}{2}(\omega^*)^2(-\ln\omega^*)+\delta)}\Big) + o(1),$$

as $\varepsilon \to 0$.

Remark 1. Since ω^ε is slightly above $\omega^* = \max_\alpha \omega^\alpha$, we have that ω^ε is located in the bandgap region. This means that the corresponding function u^ε, the solution to (7), should be localized around the defect.

4.2   Proofs of Lemma 3

Proof of (i). Recall that $(\omega^*)^2 \ln\omega^* = O(\delta)$ as $\delta \to 0$ [3]. So we need the low frequency asymptotics of the operator $\mathcal{A}^*(\omega^*, \delta)$. We use the following asymptotic expansions of the Hankel function for small arguments:

$$\big(H_0^{(1)}\big)'(z) = \frac{2i}{\pi}\frac{1}{z} - \frac{i}{\pi}z\ln z + O(z),$$

$$\big(H_0^{(1)}\big)''(z) = -\frac{2i}{\pi}\frac{1}{z^2} - \frac{i}{\pi}\ln z + O(1).$$

Straightforward computations show that, for small k,

$$\frac{d}{dk}\mathcal{S}_D^k[\phi] = \frac{1}{2\pi k}\int_{\partial D}\phi(y)d\sigma(y) - \frac{k\ln k}{4\pi}\int_{\partial D}|x-y|^2\phi(y)d\sigma(y) + O(k),$$

and

$$\frac{d}{dk}(\mathcal{K}_D^k)^*[\phi] = -\frac{k\ln k}{4\pi}\int_{\partial D}\langle x-y, \nu_x\rangle\phi(y)d\sigma(y) + O(k).$$

Also, by the symmetry argument for $\alpha^* = (\pi, \pi)$, one can see that

$$\mathcal{S}_D^{k,\alpha^*}[\phi] = \mathcal{S}_D[\phi] + O(k\ln k), \tag{26}$$

and

$$\frac{d}{dk}\mathcal{S}_D^{k,\alpha^*}[\phi] = \frac{1}{2\pi k}\int_{\partial D}\phi(y)d\sigma(y) - \frac{k\ln k}{4\pi}\int_{\partial D}|x-y|^2\phi(y)d\sigma(y) + O(k).$$

Recall that $\ker\mathcal{A}^*(\omega^*, \delta)$ is spanned by Φ^*. Let us write

$$\Phi^* = \begin{pmatrix}\varphi^*\\\psi^*\end{pmatrix},$$

and assume that Φ^* is chosen so that $\int_{\partial D}\varphi^* = 2\pi R$. Next we consider the kernel of the limiting operator of $\ker\mathcal{A}^*(\omega,\delta)$ when $\omega = 0$, $\delta = 0$, *i.e.*,

$$\mathcal{A}^*(0,0) = \begin{pmatrix}\mathcal{S}_D & -\mathcal{S}_D^{\alpha^*,0}\\-\frac{1}{2}I + \mathcal{K}_D^* & 0\end{pmatrix}.$$

It is known that $\ker(-\frac{1}{2}I + \mathcal{K}_D^*)$ is one dimensional (see, for instance, [4]). We choose an element $\varphi_0^* \in L^2(\partial D)$ such that

$$\Big(-\frac{1}{2}I + \mathcal{K}_D^*\Big)[\varphi_0^*] = 0, \quad \int_{\partial D}\varphi_0^* = 2\pi R,$$

Then we define $\psi_0^* = (\mathcal{S}_D^{0,\alpha^*})^{-1}[\mathcal{S}_D[\varphi_0]]$ and denote

$$\Phi^{0,*} = \begin{pmatrix}\varphi_0^*\\\psi_0^*\end{pmatrix}.$$

It can be shown that $\Phi^* \to \Phi^{0,*}$ as $\delta \to 0$.

Since D is a disk, $\varphi_0^* = a\chi_{\partial D}$ for some positive constant $a > 0$. Since $\int_{\partial D} \varphi_0^* = 2\pi R$ implies $a = 1$, then, by (26), we get $\psi_0^* = \chi_{\partial D} + o(1)$ as $\delta \to 0$. Therefore, for small δ, we have

$$
\begin{aligned}
\left\langle \Phi^*, \frac{d}{d\omega}\mathcal{A}^*(\omega^*,\delta)\Phi^* \right\rangle &\approx \left\langle \Phi^{0,*}, \frac{d}{d\omega}\mathcal{A}^*(\omega^*,\delta)\Phi^{0,*} \right\rangle \\
&\approx \left\langle \chi_{\partial D}, \frac{d}{d\omega}\mathcal{S}_D^{k_b}[1] \right\rangle - \left\langle \chi_{\partial D}, \frac{d}{d\omega}\mathcal{S}_D^{k_b,\alpha^*}[1] \right\rangle + \left\langle a\chi_{\partial D}, \frac{d}{d\omega}(\mathcal{K}_D^{k_b})^*[1] \right\rangle \\
&\approx -\frac{\omega^* \ln \omega^*}{4\pi} \int_{\partial D} \langle x - y, \nu_x \rangle d\sigma(y) = -\omega^* \ln \omega^* \frac{R^2}{2}.
\end{aligned}
$$

Since $\omega^* \ln \omega^* < 0$, the conclusion follows. $\qquad\square$

Proof of (ii). Using asymptotic expansions of the Bessel function $J_n(z)$ and the Hankel function $H_n^{(1)}(z)$, for small z, straightforward computations yield

$$
(\mathcal{A}_{D_d})_{V_{00}^d \to V_{00}^d} \approx \begin{pmatrix} R_d \ln R_d & -R_d \ln R_d \\ -\frac{R_d^2}{2}(\omega^*)^2 \ln \omega^* & -\delta \end{pmatrix},
$$

and

$$
(\mathcal{P}_1)_{V_{00} \to V_{00}^d} \approx \begin{pmatrix} \frac{\ln R}{\ln R_d} & 0 \\ 0 & 1 \end{pmatrix}, \quad (\mathcal{P}_2)_{V_{00}^d \to V_{00}} \approx \begin{pmatrix} 1 & 0 \\ 0 & \frac{R_d}{R} \end{pmatrix}.
$$

Therefore,

$$
\begin{aligned}
(\mathcal{A}_D^\varepsilon)_{V_{00} \to V_{00}} &= (\mathcal{P}_2^{-1}\mathcal{A}_{D_d}\mathcal{P}_1)_{V_{00} \to V_{00}} \\
&\approx \begin{pmatrix} R_d \ln R & -R_d \ln R \\ -\frac{1}{2}RR_d(\omega^*)^2 \ln \omega^* & -\delta\frac{R}{R_d} \end{pmatrix} \\
&\approx \begin{pmatrix} R \ln R & -R \ln R \\ -\frac{1}{2}R^2(\omega^*)^2 \ln \omega^* & -\delta \end{pmatrix} + \varepsilon \begin{pmatrix} \ln R & -\ln R \\ -\frac{R}{2}(\omega^*)^2 \ln \omega^* & \delta/R \end{pmatrix}.
\end{aligned}
$$

Finally, we obtain

$$
\begin{aligned}
\left\langle \Phi^*, \left(\mathcal{A}_D^\varepsilon(\omega^*,\delta) - \mathcal{A}_D(\omega^*,\delta)\right)\Phi^* \right\rangle &\approx \left\langle \begin{pmatrix} 1 \\ 1 \end{pmatrix}, \begin{pmatrix} \ln R & -\ln R \\ -\frac{1}{2}R(\omega^*)^2 \ln \omega^* & \delta/R \end{pmatrix}\begin{pmatrix} 1 \\ 1 \end{pmatrix} \right\rangle \\
&\approx 4\pi\left(-\frac{R^2}{2}(\omega^*)^2 \ln \omega^* + \delta\right).
\end{aligned}
$$

The proof is then completed. $\qquad\square$

5 Numerical illustration

Here we provide numerical examples showing the existence of the subwavelength localized modes.

Implementation. For numerical computations, we discretize the operator $\mathcal{M}^\varepsilon$ appearing in (23). Recall that it is given by

$$
\mathcal{M}^\varepsilon(\omega) = \left(I + (\mathcal{A}_D^\varepsilon(\omega,\delta) - \mathcal{A}_D(\omega,\delta))\frac{1}{(2\pi)^2}\int_{BZ}\mathcal{A}^\alpha(\omega,\delta)^{-1}d\alpha\right).
$$

We use the Fourier basis for the discretization as in [3]. Specifically, we use $e^{in\theta}, n = -N, \ldots, N$ as basis where N is the truncation order. If we increase N, then we should get more accurate results.

The operators $\mathcal{A}_D$ and $\mathcal{A}_D^\varepsilon$ are already represented in the Fourier basis in (15) and (17), respectively. We next consider the operator $\mathcal{A}^\alpha$. In [3], it was shown that, the operators $\mathcal{S}^{\alpha,k}$ and $\partial\mathcal{S}_D^{\alpha,k}/\partial\nu|_{\partial D}^{\pm}$ have the following matrix representations in the Fourier basis:

$$
\mathcal{S}_D^{\alpha,k}|_{\partial D} \approx (S_{m,n}^\alpha)_{m,n=-N}^N, \quad \frac{\partial\mathcal{S}_D^{\alpha,k}}{\partial\nu}\Big|_{\partial D}^{\pm} \approx (\widetilde{S}_{m,n}^\alpha)_{m,n=-N}^N,
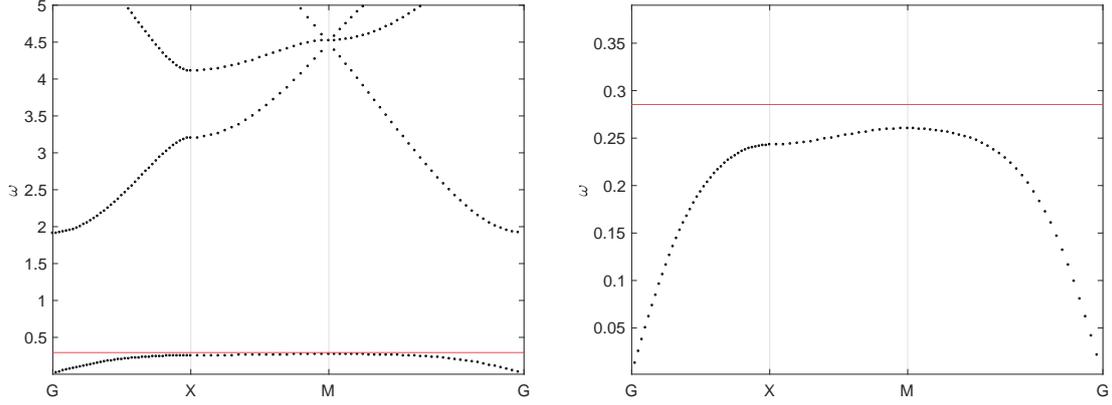$$

Figure 1: (Dilute case) The black circles represent a band structure of the unperturbed crystal with radius $R = 0.05$, $\delta = 1/5000$. The horizontal red line represents the frequency of localized mode for the perturbed crystal $\mathcal{C}_d$ with $\varepsilon = 0.03 \times R = 0.0015$.

where the matrix elements $S_{m,n}^{\alpha}$ and $\widetilde{S}_{m,n}^{\alpha}$ are given by

$$S_{m,n}^{\alpha} = -\frac{i\pi R}{2} J_n(kR) H_n^{(1)}(kR) \delta_{mn} - \frac{i\pi R}{2} J_n(kR)(-1)^{n-m} Q_{n-m} J_m(kR),$$

$$\widetilde{S}_{m,n}^{\pm} = \pm \frac{1}{2} - k \frac{i\pi R}{2} \Big(J_n \cdot (H_n^{(1)})' + J_n' \cdot H_n^{(1)} \Big)(kR) \delta_{mn} - \frac{i\pi R}{2} J_n(kR)(-1)^{n-m} Q_{n-m} k J_m'(kR). \tag{27}$$

Here, Q_n is so called the lattice sum defined by

$$Q_n := \sum_{m \in \mathbb{Z}^2, m \neq 0} H_n^{(1)}(k|m|) e^{in \arg(m)} e^{im \cdot \alpha}.$$

For an efficient method for computing the lattice sum Q_n, we refer the reader to [29]. From (27), the matrix representation of $\mathcal{A}^{\alpha}$ immediately follows.

It remains to consider the integral $\int_{BZ} (\mathcal{A}^{\alpha})^{-1} d\alpha$. We compute the two-dimensional integration with respect to α using Gauss quadruture. Then, we finally get the discretization $(M_{m,n}^{\varepsilon})$ of the operator $\mathcal{M}^{\varepsilon}(\omega)$. To find the resonant frequency for the localized mode, we apply Muller's method [6] to the determinant of the matrix $(M_{m,n}^{\varepsilon})$. The maximum frequency ω^* of the first band can be used for good initial guess.

Example 1. We first consider a dilute case where the radius of the bubble is small compared to the periodicity. We set a small radius $R = 0.05$. For the material parameters, we use $\rho_w = \kappa_w = 5000$ and $\rho_b = \kappa_b = 1$. In this case, we have $\delta = 0.0002$. In Figure 1, we show the computed band structure for this dilute case and the frequency ω^{ε} for the localized mode. Specifically, the frequency ω^{ε} is the characteristic value of $\mathcal{M}^{\varepsilon}$ near ω^*. The black circles represents the band structure of the unperturbed crystal $\mathcal{C}$. The horizontal red line corresponds to the frequency ω^{ε} for the localized mode. The band strucutre is computed in the exactly same way as in [3]. The points G, X and M represent $\alpha = (0,0)$, $\alpha = (\pi, 0)$, and $\alpha = (\pi, \pi)$, respectively. We used $N = 7$ for the truncation order of the Fourier basis.

To better illustrate the results, we also plot the magnified subwavelength band by changing the range of ω to a low frequency region $\{\omega : \omega \in (0, 0.3)\}$ (the right figure of Figure 1). In the first band, the maximum of ω is attained at the point M (or $\alpha = \alpha^* = (\pi, \pi)$). The maximum frequency ω^* of the first band is $\omega^* \approx 0.2109$. The computed frequency for the localized mode is $\omega^{\varepsilon} \approx 0.2453$. So the shift of the frequency is $\omega^{\varepsilon} \approx 0.0344 > 0$. Clearly, the frequency ω^{ε} is located slightly above the subwavelength band. As desired, the frequency ω^{ε} lies in the band gap region. Note that ω^{ε} is also in the subwavelength regime. So it indicates the existence of a subwavelength localized mode.

Example 2. Next we turn to the non-dilute case. We set a radius R as $R = 0.25$. For the material parameters, we use $\rho = \kappa = 1000$ and $\rho_b = \kappa_b = 1$. So we have $\delta = 0.001$. In Figure 2, we show the computed band structure for this non-dilute case. The maximum frequency ω^* of the first band is $\omega^* \approx 0.2109$. The computed frequency ω^{ε} for the localized mode is $\omega^{\varepsilon} \approx 0.2453$. So the shift of the
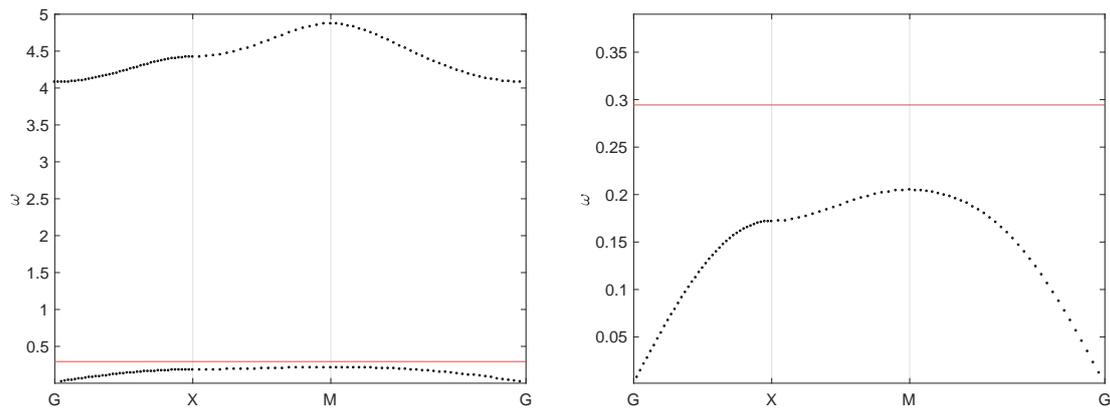
Figure 2: (Non-dilute case) The black circles represent a band structure of the unperturbed crystal with radius $R = 0.25$, $\delta = 1/1000$. The horizontal red line represents the frequency of localized mode for the perturbed crystal $\mathcal{C}_d$ with $\varepsilon = 0.03 \times R = 0.0075$.

frequency is $\omega^\varepsilon - \omega^* \approx 0.0344 > 0$. Again, the frequency ω^ε is located above the subwavelength band. We used $N = 3$ for the truncation order.

6   Concluding remarks

In this paper, we have proved for the first time the possibility of localizing waves at the deep subwavelength scale. We have considered a bubbly crystal and produced a localized mode by increasing the size of one bubble. We have illustrated our findings with numerical experiments. Our results in this paper shed light on the mechanism behind the control and guiding of waves at deep subwavelength scales. In forthcoming works, we plan to investigate the robustness of such subwavelength defect modes with respect to spatial disorder. We will also consider the possibility of guiding waves at deep subwavelength scales using line defects. Another challenging problem we plan to tackle is to prove or disprove the existence of fundamental limits on the Purcell factor in subwavelength bandgap materials.

References

[1] H. Ammari, B. Fitzpatrick, D. Gontier, H. Lee, and H. Zhang. Minnaert resonances for acoustic waves in bubbly media. *Annales de l'Institut Henri Poincaré: Analyse Nonlinéaire, to appear.*

[2] H. Ammari, B. Fitzpatrick, D. Gontier, H. Lee, and H. Zhang. Sub-wavelength focusing of acoustic waves in bubbly media. *Proc. Royal Soc. A*, 473:20170469, 2017.

[3] H. Ammari, B. Fitzpatrick, H. Lee, S. Yu, and H. Zhang. Subwavelength phononic bandgap opening in bubbly media. *J. Differential Equations*, 263(9):5610–5629, 2017.

[4] H. Ammari and H. Kang. *Polarization and moment tensors: with applications to inverse problems and effective medium theory*, volume 162. Springer Science & Business Media, 2007.

[5] H. Ammari, H. Kang, and H. Lee. Asymptotic analysis of high-contrast phononic crystals and a criterion for the band-gap opening. *Arch. Ration. Mech. Anal.*, 193(3):679–714, 2009.

[6] H. Ammari, H. Kang, and H. Lee. *Layer Potential Techniques in Spectral Analysis*, volume 153 of *Mathematical Surveys and Monographs*. American Mathematical Society, Providence, 2009.

[7] H. Ammari, H. Kang, S. Soussi, and H. Zribi. Layer potential techniques in spectral analysis. ii. sensitivity analysis of spectral properties of high contrast band-gap materials. *Multiscale Model. Simul.*, 5(2):646–663, 2006.

[8] H. Ammari, H. Lee, and H. Zhang. High frequency homogenization of bubbly crystals. *arXiv, 1708.07955.*

[9] H. Ammari and H. Zhang. A mathematical theory of super-resolution by using a system of sub-wavelength Helmholtz resonators. *Commun. in Math. Phys.*, 337(1):379–428, 2015.

[10] H. Ammari and H. Zhang. Super-resolution in high-contrast media. *Proc. R. Soc. A*, 471(2178), 2015.

[11] Habib Ammari and Fadil Santosa. Guided waves in a photonic bandgap structure with a line defect. *SIAM J. Appl. Math.*, 64(6):2018–2033, 2004.

[12] V. Duchêne, I. Vukićević, and M.I. Weinstein. Oscillatory and localized perturbations of periodic structures and the bifurcation of defect modes. *SIAM J. Math. Anal.*, 47(5):3832–3883, 2015.

[13] Vincent Duchêne, Iva Vukićević, and Michael I. Weinstein. Homogenized description of defect modes in periodic structures with localized defects. *Commun. Math. Sci.*, 13(3):777–823, 2015.

[14] A. Figotin and V. Goren. Resolvent method for computations of localized defect modes of H-polarization in two-dimensional photonic crystals. *Phys. Rev. E*, 64(3):056623, 16 pp, 2001.

[15] A. Figotin and A. Klein. Midgap defect modes in dielectric and acoustic media. *SIAM J. Appl. Math.*, 58(6):1748–1773, 1998.

[16] Alexander Figotin and Abel Klein. Localized classical waves created by defects. *Journal of Statistical Physics*, 86(1):165–177, Jan 1997.

[17] F. Figotin and P. Kuchment. Spectral properties of classical waves in high-contrast periodic media. *SIAM J. Appl. Math.*, 58(2):683–702, 1998.

[18] I.C. Gohberg and E.I. Sigal. An operator generalization of the logarithmic residue theorem and the theorem of Rouché. *Sb. Math.*, 13(4):603–625, 1971.

[19] R. Hempel and K. Lienau. Spectral properties of periodic media in the large coupling limit. *Comm. Partial Differential Equations*, 25:1445–1470, 2000.

[20] M.A. Hoefer and M.I. Weinstein. Defect modes and homogenization of periodic Schrödinger operators. *SIAM J. Math. Anal.*, 43(2):971–996, 2011.

[21] A. Klein and A. Koines. A general framework for localization of classical waves. I. Inhomogeneous media and defect eigenmodes. *Math. Phys. Anal. Geom.*, 4(2):97–130, 2001.

[22] P. Kuchment. *Floquet Theory for Partial Differential Equations.* Number 60 in Operator Theory: Advances and Applications. Birkhäuser Verlag, Basel, 1993.

[23] Peter Kuchment. An overview of periodic elliptic operators. *Bull. Amer. Math. Soc.*, 53(3):343–414, 2016.

[24] Fabrice Lemoult, Nadège Kaina, Mathias Fink, and Geoffroy Lerosey. Wave propagation control at the deep subwavelength scale in metamaterials. *Nature Physics*, 9:55–60, 2013.

[25] Fabrice Lemoult, Nadège Kaina, Mathias Fink, and Geoffroy Lerosey. Soda cans metamaterial: A subwavelength-scaled phononic crystal. *Crystals*, 6(7), 2016.

[26] J. Lin. A perturbation approach for near bound-state resonances of photonic crystal with defect. *European J. Appl. Math.*, 27(1):66–86, 2016.

[27] Junshan Lin and Fadil Santosa. Resonances of a finite one-dimensional photonic crystal with a defect. *SIAM J. Appl. Math.*, 73(2):1002–1019, 2013.

[28] S.-Y. Lin, E. Chow, V. Hietala, P.R. Villeneuve, and J.D. Joannopoulos. Experimental demonstration of guiding and bending of electromagnetic waves in a photonic crystal. *Science*, 282:274–276, 1998.

[29] C. M. Linton. Lattice sums for the helmholtz equation. *SIAM Rev.*, 52(4):630–674, 2010.

[30] Robert Lipton and Robert Jr. Viator. Creating band gaps in periodic media. *Multiscale Model. Simul.*, 15(4):1612–1650, 2017.

[31] Robert Lipton and Robert Jr. Viator. Bloch waves in crystals and periodic high contrast media. *ESAIM Math. Model. Numer. Anal.*, 51(3):889–918, 2017.

[32] Z. Liu, , X. Zhang, Y. Mao, Y.Y. Zhu, Z. Yang, C.T. Chan, and P. Sheng. Locally resonant sonic materials. *Science*, 289(5485):1734–1736, 2000.

[33] K.H. Matlack, A. Bauhofer, S. Krödel, A. Palermo, and C. Daraio. Composite 3d-printed metastructures for low-frequency and broadband vibration absorption. *Proc. Natl. Acad. Sci. USA*, 113(30):8386–8390, 2016.

[34] M. Minnaert. On musical air-bubbles and the sounds of running water. *The London, Edinburgh, Dublin Philos. Mag. and J. of Sci.*, 16:235–248, 1933.

[35] E.M. Purcell. Spontaneous emission probabilities at radio frequencies. *Phys. Rev.*, 69:674, 1946.

[36] E.L. Thomas. Bubbly but quiet. *Nature*, 462(24), 2009.

[37] S. Wilcox, L. C. Botten, R. C. McPhedran, C. G. Poulton, and C. Martijn de Sterke. Modeling of defect modes in photonic crystals using the fictitious source superposition method. *Phys. Rev. E*, 71:056606, May 2005.